MAPK Signal-integrating Kinase Controls Cap-independent Translation and Cell Type-specific Cytotoxicity of an Oncolytic Poliovirus

Christian Goetz[1], Richard G Everson[1], Linda C Zhang[1] and Matthias Gromeier[1]

[1]*Division of Neurosurgery, Department of Surgery, Duke University Medical Center, Durham, North Carolina, USA*

Many animal viruses exhibit proficient growth in transformed cells, a property that has been harnessed for the development of novel therapies against cancer. Despite overwhelming evidence for this phenomenon, understanding of the molecular mechanisms enabling tumor-cell killing is rudimentary for most viruses. We report here that growth and cytotoxicity of the prototype oncolytic poliovirus (PV), PVSRIPO, in glioblastoma multiforme (GBM) is promoted by mitogen-activated protein kinases (MAPKs) converging on the MAPK signal-integrating kinase 1 (Mnk1) and its primary substrate, the eukaryotic initiation factor (eIF) 4E. Inducing Mnk1-catalyzed eIF4E phosphorylation through expression of oncogenic Ras substantially enhanced PVSRIPO translation, replication, and cytotoxicity in resistant cells. This effect was mimicked by expression of constitutively active forms of Mnk1 and correlated with enhanced translation of subgenomic reporter RNAs. Our findings implicate Mnk1 activity in stimulation of PVSRIPO cap-independent translation, an effect that can be synergistically enhanced by inhibition of the phosphoinositide-3 kinase (PI3K).

Received 20 May 2010; accepted 14 June 2010; published online 20 July 2010. doi:10.1038/mt.2010.145

INTRODUCTION

Poliovirus (PV) has been engineered for selective replication in neoplastic cells by exchange of its cognate internal ribosomal entry site (IRES) with that of human rhinovirus type 2 (HRV2).[1] This diminishes replication potential in cells of neuronal derivation, *e.g.*, neuroblastoma cell lines[2] or human embryonic kidney 293 (HEK-293) neuroblastic cells[3,4] and eliminates the inherent neuropathogenicity associated with PV infection. The prototype oncolytic PV/HRV chimera, PVSRIPO, was devoid of pathogenic properties after intracerebral inoculation of 5×10^9 tissue culture infectious doses in an investigational new drug-directed dose-range finding, toxicology, and biodistribution study in *Macaca fascicularis* (personal communication). Yet, despite neuronal incompetence of PVSRIPO, it is associated with significant cytotoxicity and progeny production in neoplastic cells, *e.g.*, cell lines derived of malignant glioma.[1]

This suggests that conditions restricting PVSRIPO in the normal central nervous system are absent in glioblastoma multiforme (GBM) and that the cell type-specific environment in GBM favors viral growth. Indeed, PVSRIPO retained its highly neuroattenuated genotype after serial passage in GBM xenografts *in vivo*, suggesting optimal conditions for function of the heterologous 5′ untranslated region driving viral RNA translation and propagation.[5] Unraveling the mechanism responsible for PVSRIPO cytotoxicity in GBM is of key interest because PVSRIPO oncolysis categorically depends on IRES-mediated protein synthesis and understanding the regulation of viral IRES function may shed light on control of translation initiation in cancer.

Conventional translation initiation occurs upon eukaryotic initiation factor (eIF)4E binding the m^7G-cap on eukaryotic mRNAs[6] along with eIF4G,[7,8] a scaffold protein which attracts 40S ribosomal subunits through binding the multisubunit eIF3 complex. The principle of cap-independent, IRES-mediated translation was first discovered with picornaviruses,[9,10] whose (+)strand RNA genomes are naturally uncapped.[11] Translation initiation at picornaviral RNAs bypasses eIF4E and occurs via binding of eIF4G directly to the IRES.[12,13] Malignant transformation entails profound changes to protein synthesis machinery. Notably, this entails post-translational modification of translation factors that regulate ribosome recruitment to mRNAs. For example, activation of the phosphoinositide-3 kinase (PI3K) pathway leads to phosphorylation of eIF4E-binding proteins (4E-BPs)[14] and eIF4G[15] via the mammalian target of rapamycin (mTOR). The 4E-BPs preclude eIF4E–4G interaction and decrease cap-dependent translation,[16] but their eIF4E-binding capacity is reversed upon phosphorylation. Activation of the mitogen-activated protein kinases (MAPKs) Erk1/2 or p38 induces eIF4E phosphorylation at Ser209 via their common substrate, Mnk.[17,18] In order to phosphorylate eIF4E, Mnk must associate with eIF4G.[19]

To provide correlative mechanistic support for PVSRIPO, we investigated the effect of oncogenic signaling on virus-mediated cancer-cell killing. PVSRIPO translation, growth, and cytotoxicity are responsive to major mitogenic signaling pathways via PI3K/mTOR and Ras/MAPK. PVSRIPO oncolysis is enabled by Ras/MAPK signaling and the MAPK substrate Mnk1 in particular. Mnk1 is a convergence node for multiple major signal transduction pathways and is broadly activated in GBM, tumors with

Correspondence: *Matthias Gromeier, Division of Neurosurgery, Department of Surgery, Duke University Medical Center, Durham, North Carolina 27710, USA. E-mail: grome001@mc.duke.edu*

universally active Erk1/2 and p38-MAPK signaling. Based on our findings, we propose that signal transduction to Mnk1 favors viral, cap-independent translation, enabling efficient PVSRIPO propagation and cytotoxicity. This effect can be further enhanced by concomitant inhibition of PI3K, potentially due to stimulation of cap-independent translation via inhibition of the mammalian target of rapamycin (mTOR) and resulting dephosphorylation of 4E-BPs.[20]

RESULTS

Oncogenic signaling modulates PVSRIPO cytotoxicity

GBM is associated with alteration of genes encoding proteins involved in mitogenic signal transduction, producing widespread active PI3K/Akt and Ras/MAPK signaling.[21] Hence, U-118 glioma cells grown in the presence of serum exhibit phosphorylation of downstream PI3K and Ras/MAPK effectors (**Figure 1a**). U-118, like other glioma cell lines, is highly susceptible to PVSRIPO propagation and cytotoxicity.[5] Serial passage of PVSRIPO in U-118 xenografts produced potent oncolysis without evidence for genetic adaptation of the virus, indicating proper function of the engineered 5′ untranslated region in such cells.[5] To investigate the molecular mechanisms permitting optimal growth of PVSRIPO in glioma cells, we tested the influence of oncogenic signals on viral translation and growth. To this end, we used inhibitors of PI3K (LY294002), Mek1/2 (UO126) and its substrate Mnk1 (CGP57380) (**Figure 1a**). All inhibitors had the expected effects in U-118 cells. UO126, while inhibiting phosphorylation of the Mek substrates Erk1/2 effectively, failed to block eIF4E phosphorylation (**Figure 1a**), although the eIF4E kinase Mnk1 is an Erk1/2 substrate (**Figure 1a**). This is explained by active p38 MAPK, which also feeds into Mnk1 signaling to eIF4E[18] (**Figure 1a**). In contrast, CGP57380 inhibits Mnk1 directly, blocking eIF4E phosphorylation in a dose-responsive manner (**Figure 1a**).

U-118 cells were vehicle-treated or treated with the appropriate compounds for 2 hours and infected with PVSRIPO at a multiplicity of infection (MOI) of 10 (**Figure 1b**). Progeny (plaque-forming units) and the viral nonstructural proteins 2C/2BC were analyzed at the indicated intervals. PI3K inhibition accelerated the onset of viral translation and growth slightly, but reproducibly, by ~1 hour (**Figure 1b**). Interestingly, CGP57380 substantially repressed viral growth. The onset of viral translation was delayed by 2 hours and peak production of progeny was reduced by ~60% (**Figure 1b**). Conversely, UO126 failed to significantly alter viral replication (**Figure 1b**). Correlation of PVSRIPO propagation and

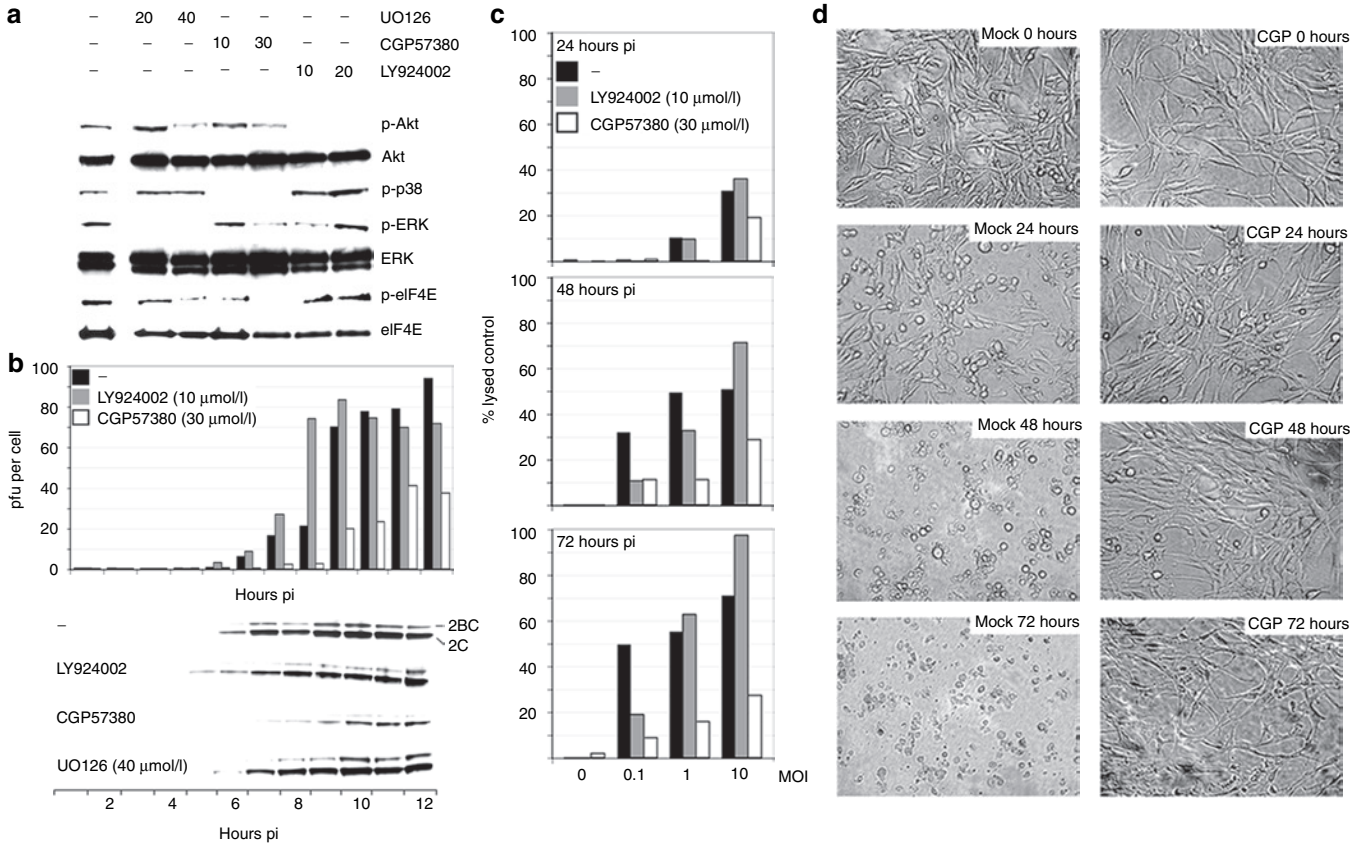

Figure 1 Protein kinase inhibitors modulate PVSRIPO oncolysis in U-118 cells. (**a**) Immunoblots of kinase substrates in the PI3K- (Akt) and MAPK pathways (p38, Erk, eIF4E) 2 hours after treatment with vehicle (–), UO126, CGP57380, or LY924002 (concentrations in µmol/l are shown atop). (**b**) Kinetics of viral growth (top) and translation (bottom) in mock- or inhibitor-treated U-118 cells infected with PVSRIPO (MOI = 10). Progeny was quantified by plaque assay and viral translation was measured by immunoblot of the viral nonstructural proteins 2BC/2C. Viral propagation in mock- and UO126-treated cells was similar (data not shown). (**c**) PVSRIPO cytotoxicity in mock- or inhibitor-treated U-118 cells at the indicated intervals. (**d**) Photomicrographs of PVSRIPO-infected (MOI = 1), vehicle- (mock) or CGP57380 (CGP; 30 µmol/l)-treated U-118 cells at the indicated intervals. MAPK, mitogen-activated protein kinase; MOI, multiplicity of infection; pfu, plaque-forming units.

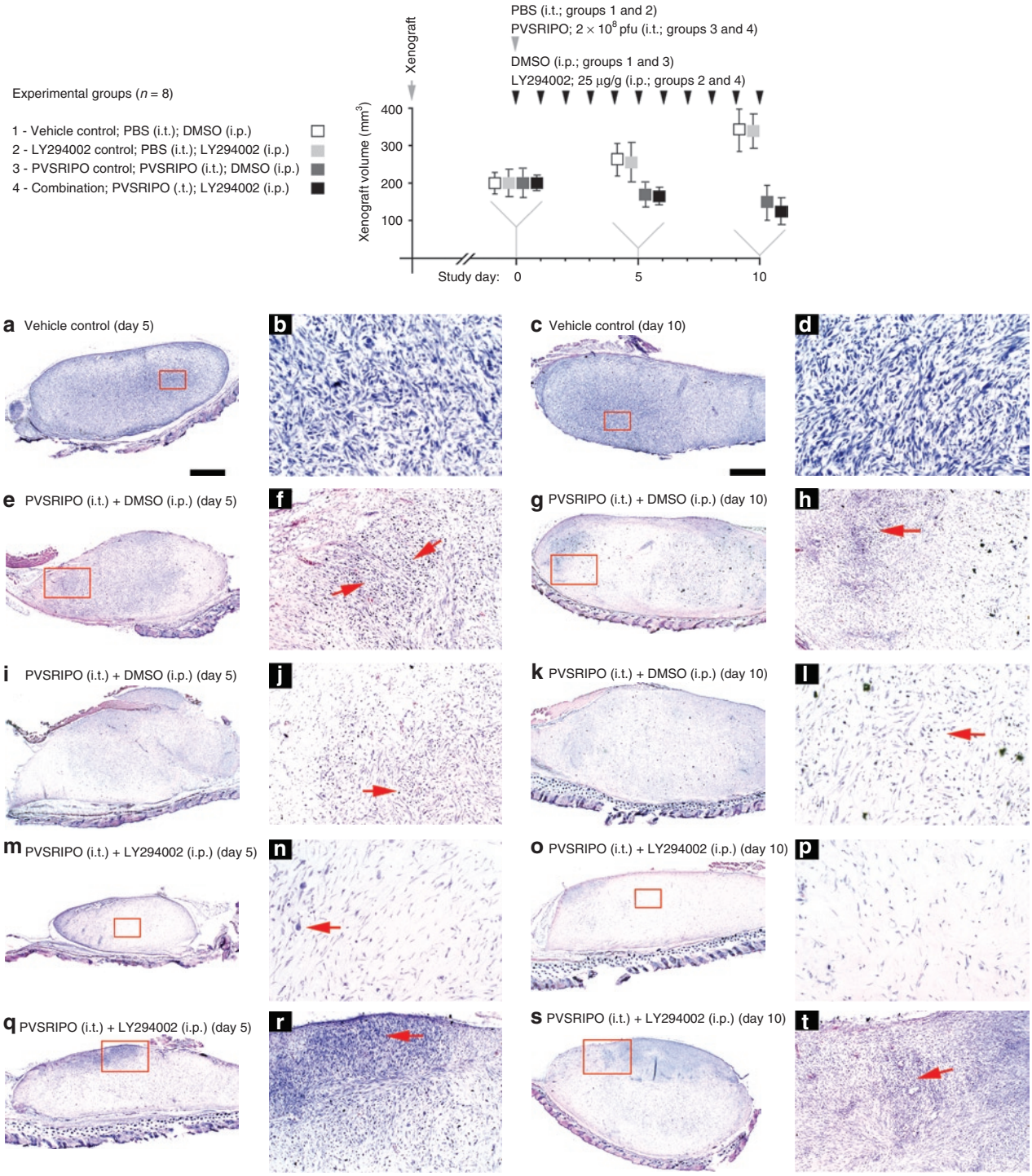

Figure 2 Testing PVSRIPO and PI3K inhibitor synergy *in vivo*. Experimental groups and the study regimen are indicated atop. U-118 xenografts were measured at study days 0 (when PVSRIPO/vehicle and LY294002/vehicle treatment was initiated), 5, and 10. Four animals of each group were euthanized at study days 5 and 10 for histology and virus recovery. The bottom panels show histology from xenografts recovered at day 5 (left columns) and 10 (right columns). Tumors from one animal in group 1 at (**a**,**b**) day 5 and (**c**,**d**) day 10, two animals in group 3 at (**e**,**f**,**i**,**j**) day 5 and (**g**,**h**,**k**,**l**) day 10 and two animals in group 4 at (**m**,**n**,**q**,**r**) day 5 and (**o**,**p**,**s**,**t**) day 10 were analyzed. Low-magnification images in the left columns are accompanied by higher magnification images from the same section (red inserts) in the column to their right. (**a**–**d**) Tumor histology of a representative xenograft from group 1 shows the characteristic dense arrangement of tumor cells. (**e**–**l**) Histology of two representative tumors from group 3 at study days 5 and 10 as indicated. Note extensive tumor cell loss and "empty" appearance of the former xenograft in all cases. Red arrows point to areas of intense tumor-cell killing and active tissue rearrangement. (**m**–**t**) Histology of four representative tumors from group 4 at study days 5 and 10 as indicated. (**m**,**n**,**o**,**p**) show almost complete tumor regress at study days 5 and 10. (**n**,**p**) The area of the former tumor was invaded by cells with fibroblast morphology surrounded by dense extracellular matrix. Isolated viable tumor cells (**n**; arrow) may remain. (**q**,**r**) Active tumor (red arrow), which was still present in three animals of group 4 at day 5 and two animals at (**s**,**t**) day 10. DMSO, dimethyl sulfoxide; i.p., intraperitoneal; i.t., intratumoral; PBS, phosphate-buffered saline.

cytotoxicity with eIF4E phosphorylation in U-118 cells suggested involvement of the eIF4E kinase Mnk in virus susceptibility.

As PVSRIPO is under consideration for clinical use because of its specific cytotoxic properties, we evaluated the effects of kinase inhibitors on infected glioma cells using a lactate-dehydrogenase-based cytotoxicity assay (**Figure 1c**). U-118 cells were infected at varying MOIs and treated with CGP57380 or LY294002 (**Figure 1c**). Tests of mock-infected cells showed that neither drug caused significant cytotoxicity on its own during the course of the assay (**Figure 1c**). Mock-treated cells exhibited significant PVSRIPO cytotoxicity at all intervals (**Figure 1c**) and cell killing was complete before 48 hours (**Figure 1d**). CGP57380 exhibited a marked cytoprotective effect, reducing virus-mediated cytotoxicity by ~70% at the highest MOI at 72-hour interval (**Figure 1c**). Accordingly, CGP57380 prevented cytopathogenic changes of cell morphology typical for PVSRIPO. At an MOI of 1, cell killing was abrogated almost entirely (**Figure 1d**). PI3K inhibition modestly increased cytopathogenicity at MOIs >1 (**Figure 1c**).

PI3K inhibition promotes PVSRIPO oncolysis *in vivo*

Since PI3K inhibition promoted viral translation, accelerated virus propagation, and stimulated PVSRIPO cytotoxicity (at MOIs >1), it may be used synergistically in clinical applications. Thus, we evaluated combination of PVSRIPO with LY294002 *in vivo*. We used a study template employed before, consisting of bilateral U-118 glioma xenografts in athymic mice treated with intratumoral inoculation of PVSRIPO (**Figure 2**; top panels).[5] At days 5 and 10 postinfection, animals were euthanized and the excised tumors were used for histologic analyses and virus recovery. Groups of four xenografted athymic mice each received intratumoral vehicle (phosphate-buffered saline (PBS)) or PVSRIPO (2.5×10^8 plaque-forming units) into subcutaneous ~200 mm^3 xenografts (**Figure 2**). On the day of virus injection, a regimen of daily intraperitoneal injections of 25 μg/g LY294002 dissolved in dimethyl sulfoxide or dimethyl sulfoxide alone was initiated (**Figure 2**). This dose/regimen has previously been shown to produce sustained PI3K inhibition in similar animal tumor models.[22]

As reported before,[5] we observed modest reduction in tumor size in PVSRIPO-treated animals (**Figure 2**; top panels). In accordance with prior published work, LY294002 had no significant effect on tumor growth alone[23,24] or in combination with PVSRIPO (**Figure 2**; top panels). Previous research indicated that the true oncolytic potential of PVSRIPO is evident only through histological analysis.[5] Xenografts from all mice in the study where fixed, paraffin-embedded, sectioned, and hematoxylin and eosin stained in their entirety (**Figure 2a–t**). Tumors from group 1 (vehicle/dimethyl sulfoxide control) displayed typical histology at days 5 and 10 (**Figure 2a–d**). As seen before, PVSRIPO alone elicited widespread tumor-cell killing evident at days 5 and 10 (**Figure 2e–l**).[5] This was accompanied by remarkably efficient tumor loss and profound tissue rearrangements (**Figure 2e–l**). At day 5, tumor debris removal, fibroblast invasion, and scar formation were significantly enhanced in all PVSRIPO-treated animals receiving LY294002 (**Figure 2m,n,q,r**). Tumor loss was near complete in one animal of the group (**Figure 2m,n**). At study day 10, PVSRIPO-treated animals displayed prominent signs of

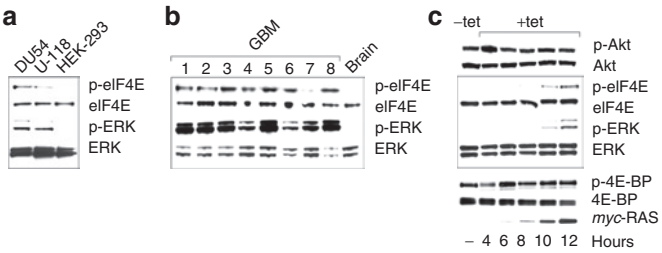

Figure 3 MAPK signaling in HEK-293 cells. (**a**) PI3K and Ras/MAPK pathways in HEK-293 cells. Erk1/2 signaling and phospho-eIF4E in HEK-293 cells is reduced compared to DU54 and U-118 GBM cells. (**b**) Universally active Erk1/2 MAPK signal and eIF4E phosphorylation in GBM patients and absent signal in the normal primate brain. (**c**) Tet induction of HEK-293^{Ras} cells produces Erk1/2 and eIF4E phosphorylation and a signaling signature similar to U-118 GBM cells or GBM patient tissues. GBM, glioblastoma multiforme; HEK-293, human embryonic kidney 293; MAPK, mitogen-activated protein kinase; tet, tetracycline.

tumor-cell killing and tissue rearrangement and a synergistic effect of LY294002 was less evident (**Figure 2**). Xenograft extinction and scar formation beyond 10 days post-PVSRIPO inoculation has been documented previously[5] and tumor regress was not followed beyond 10 days in this study.

Xenografts contralateral to the histologically analyzed tumors were homogenized and the lysate used to perform plaque assays to determine PVSRIPO content at study day 5. All xenografts from group 3 contained virus and the average titers recovered where 9.8 plaque-forming units/mg tumor. In contrast, tumors from group 4 were virus-free in three cases and the titer from the remaining animal was 0.97 plaque-forming units/mg. Because PVSRIPO recovery correlates with the presence of viable tumor in xenografts,[5] approximately tenfold reduced titers in group 4 tumors indicate diminished live cells in the xenograft. The tumor lysates were also used to confirm PI3K inhibition, evident through reduced phospho-S6 levels in groups 2 and 4 tumors (data not shown). Our data suggest that, in accordance with tissue culture findings, LY294002 synergistically accelerated PVSRIPO tumor-cell killing and xenograft regression.

H-Ras rescues PVSRIPO growth in a nonpermissive cell line

Although PVSRIPO responds positively to inhibition of PI3K/mTOR signaling *in vitro* (**Figure 1b,c**) and *in vivo* (**Figure 2**), a far more pronounced negative effect was achieved with inhibition of the Erk1/2 and p38-MAPK substrate Mnk (**Figure 1b–d**). The latter observation is of key importance, because MAPK activity may constitute a critical determinant for PVSRIPO tumor-specific growth and, thus, oncolytic efficacy. Unraveling signaling pathways that enable translation via the heterologous HRV2 IRES in PVSRIPO may also provide correlative mechanistic evidence for rational patient selection.

To further delineate the potential role for MAPK in viral oncolysis, we tested parameters for viral growth and cytotoxicity in a cell line naturally resistant to PVSRIPO. HEK-293 cells barely support PVSRIPO growth,[3] block polysome association of viral RNA[25] and resist PVSRIPO cytotoxicity.[4] To establish if this phenotype correlates with a distinct signaling status, we analyzed PI3K/Akt and MAPK signaling in HEK-293 cells (**Figure 3a**).

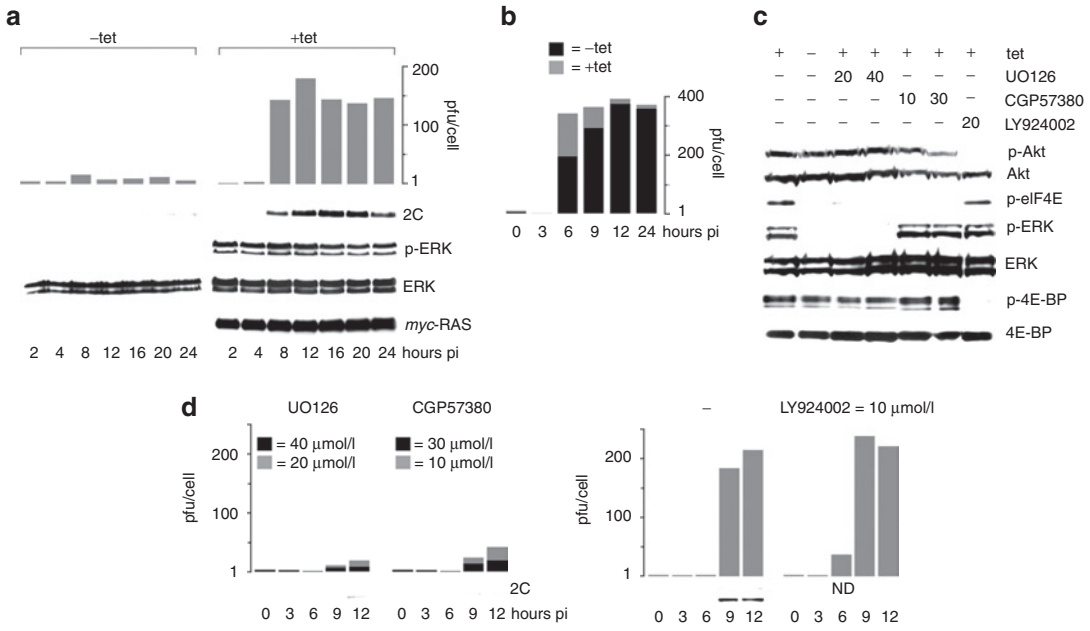

Figure 4 Oncogenic H-Ras rescues PVSRIPO growth in nonpermissive HEK-293 cells. (**a**) PVSRIPO growth (top) and translation (bottom) in mock- or tet-induced HEK-293^{Ras} cells. Immunoblots confirm *myc*-Ras expression and Erk1/2 signaling. (**b**) PV1S progeny recovered from infected (MOI = 10) mock- or tet-induced HEK-293^{Ras} cells at the indicated intervals. (**c**) Protein kinase inhibitor profiles in tet-induced HEK-293^{Ras} cells (concentrations in µmol/l are shown atop). (**d**) Effect of kinase inhibitors on PVSRIPO translation and propagation in tet-induced HEK-293^{Ras} cells. HEK-293, human embryonic kidney 293; MOI, multiplicity of infection; pfu, plaque-forming units.

Compared to established GBM cell lines, *e.g.*, DU54 or U-118, HEK-293 cells show relatively reduced Erk1/2 and p38-MAPK activity resulting in low levels of phospho-eIF4E (**Figure 3a**). This implies inherently low Mnk1 activity. This was confirmed in a HEK-293 reference cell line (ATCC, Manassas, VA; **Figure 2a**), a master HEK-293 cell bank used to establish an *in vitro* release assay for PVSRIPO at NCI[4] (Magenta, Rockville, MD) and a commercially available, tetracycline (tet)-regulated expression system (TREx; obtained from Invitrogen, Carlsbad, CA). Comparatively low Mnk1 activity in HEK-293 cells contrasts with rampant Erk1/2 activity and eIF4E phosphorylation in GBM patients, implying universally active Mnk1 in these tumors (**Figure 3b**). Detecting phospho-Mnk1 directly in patient samples is difficult due to high-inherent background signal with the only available phospho(Thr197/202)-specific antibody. Because eIF4E phosphorylation categorically depends on Mnk,[26] it is a reliable marker for Mnk activity.

To test whether Mnk1 signals rescue PVSRIPO growth in HEK-293 cells, we constructed a tet-inducible HEK-293 cell line expressing myc-tagged oncogenic (V12) Harvey (H)-Ras (HEK-293^{Ras}; **Figure 3c**). Tet induction produced abundant phoshpo-Erk1/2 and -eIF4E without effects on the PI3K/Akt pathway (**Figure 3c**). PVSRIPO translation and growth in HEK-293^{Ras} cells was potently stimulated upon tet induction. Expression of viral 2C protein was detected as early as 8 hours and titers increased ~100-fold over 12 hours compared to ~3.5-fold in mock-induced cells (**Figure 4a**). The stimulatory effect of oncogenic Ras also occurred with the PVSRIPO parent, type 1 (Sabin) PV vaccine (PV1S) in HEK-293^{Ras} cells (**Figure 4b**). PV1S propagation in plain HEK-293 cells is vastly superior to PVSRIPO[3,4] and proportionally, PV1S growth was stimulated less than PVSRIPO. Thus, the effect of oncogenic Ras may be limited by the intrinsic capacity of host cells to support PV replication.

To directly implicate MAPKs in PVSRIPO growth stimulation, tet-induced HEK-293^{Ras} cells were treated with kinase inhibitors before infection. UO126, CGP57380, and LY294002 had the anticipated effects on signaling (**Figure 4c**). Importantly, in contrast to U-118 cells, UO126 blocked PVSRIPO propagation in tet-induced HEK-293^{Ras} cells almost completely (**Figure 4d**). As with U-118 cells, CGP57380 potently reduced viral translation and proliferation in tet-induced HEK-293^{Ras} cells (**Figure 4d**). We also observed modestly enhanced early viral propagation with LY294002, previously noted in U-118 cells (**Figure 4d**). Our data show that Ras/MAPK signaling elevated deficient PV growth mediated by a heterologous HRV2 IRES or cognate PV1S IRES in HEK-293 cells. Erk1/2 inhibition blocked replication in HEK-293^{Ras} cells, but did not affect PVSRIPO growth or translation in U-118 cells (**Figures 1b** and **4d**). This discordance correlates with UO126-resistant eIF4E phosphorylation in the latter (due to simultaneous activity of p38 MAPK; **Figure 1a**) and implicates Mnk1 in PVSRIPO growth stimulation.

Oncogenic Ras does not influence PVSRIPO entry

Pleiotropic H-Ras may affect PVSRIPO propagation at multiple levels. In particular, studies with transfection of promoter reporters suggested that active Ras may upregulate the PV receptor, nectin-like molecule 5 (Necl-5).[27] Stimulation of PVSRIPO entry by oncogenic Ras via enhanced receptor expression is unlikely, because Necl-5 is exceedingly abundant in plain HEK-293 cells[4] and, since wild-type PV or PV1S grow efficiently in these cells,[3] is not a factor limiting susceptibility. Accordingly, analyses of Necl-5

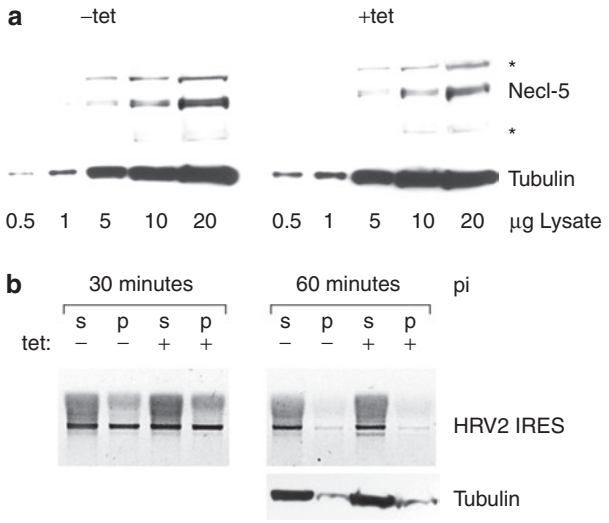

Figure 5 Necl-5 and viral entry in HEK-293^{Ras} cells. (**a**) Expression of the poliovirus receptor Necl-5 in mock- or tet-induced HEK-293 cells. The asterisks indicate nonspecific background bands. (**b**) Soluble cytoplasmic (s) and precipitated membraneous (p) fractions from mock- or tet-induced HEK-293^{Ras} cells at 30 and 60 minutes postinfection with PVSRIPO. Total RNA recovered from the cell fractions was subjected to RT-PCR analysis of PVSRIPO RNA, amplifying the heterologous IRES insert. HEK-293, human embryonic kidney 293; HRV2, human rhinovirus type 2; IRES, internal ribosomal entry site; Necl-5, nectin-like molecule 5; RT-PCR, real time-PCR.

levels in mock- and tet-induced HEK-293^{Ras} cells did not reveal Necl-5 induction upon tet-induced Ras expression (**Figure 5a**). Also, probing for viral RNA in membrane-associated and cytoplasmic fractions of HEK-293^{Ras} cells did not show any effect of oncogenic Ras on entry (**Figure 5b**).

Active Mnk1 is sufficient to increase PVSRIPO susceptibility

We were unable to test PVSRIPO cytotoxicity in tet-induced HEK-293^{Ras} cells, because prolonged H-Ras expression caused significant toxicity on its own. To resolve this issue and to test directly whether MAPKs and their Mnk1 substrate control PVSRIPO cytopathogenicity in GBM, we constructed HEK-293 cell lines expressing constitutively active (T332D) or kinase dead (T2A2) Mnk1 mutants[18] in a tet-inducible manner. Tet induction of HEK-293^{T332D} cells greatly enhanced eIF4E phosphorylation (which also occurs in uninduced cells, presumably due to leaky transcription), whereas all eIF4E phosphorylation was absent in HEK-293^{T2A2} cells (**Figure 6a**). After PVSRIPO infection at MOIs of 0.1–10, HEK-293^{T332D} cells were significantly more susceptible to PVSRIPO cytotoxicity then HEK-293^{T2A2} cells (**Figure 6b**). Treatment of HEK-293^{T332D} with CGP57380 nearly abolished this differential up to 48 hours and significantly reduced viral cytotoxicity at 72 hours postinfection (**Figure 6b**). Partial recovery of cytotoxicity in the presence of CGP57380 may be due to degradation of the compound by 72 hours.

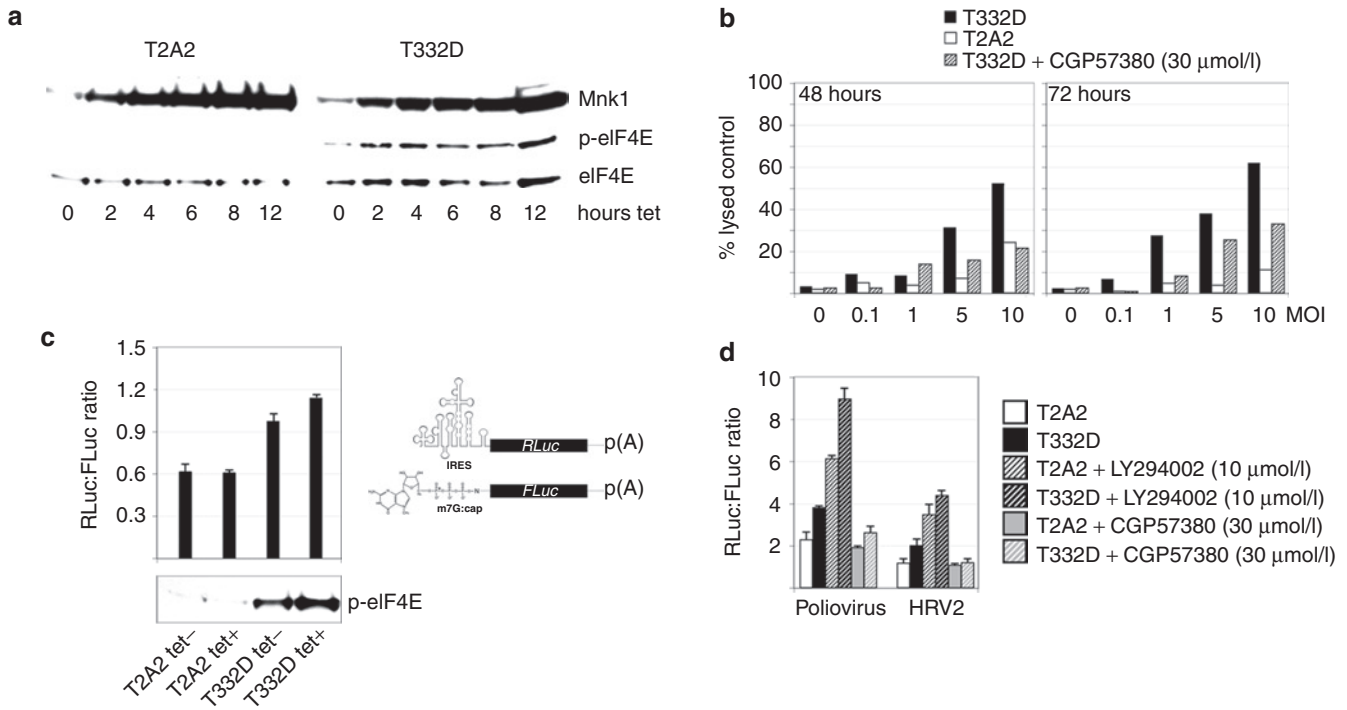

Figure 6 Mnk1 activity determines PVSRIPO cytotoxicity in HEK-293 cells and stimulates IRES-dependent translation. (**a**) Mnk1 signaling to eIF4E in tet-induced HEK-293^{T2A2} and HEK-293^{T332D} cells. (**b**) LDH cytotoxicity assay in tet-induced HEK-293^{T2A2} and HEK-293^{T332D} cells in the presence or absence of CGP57380 as indicated. (**c**) RNA co-transfection of m^{7}G-cap-leader (driving FLuc) or HRV2 IRES-driven (RLuc) reporters into mock- or tet-induced HEK-293^{T2A2} or HEK-293^{T332D} cells. IRES-dependent RLuc units were normalized to cap-dependent FLuc values. (Bottom) Phospho-eIF4E immunoblot from RNA-transfected cells. Error bars correspond to SD between triplicates. (**d**) Co-transfection of m^{7}G-cap-leader or PV1S/HRV2 IRES-dependent RNA reporters into mock- or tet-induced 293$^{T2A2/T332D}$ cells treated with vehicle or kinase inhibitors as indicated. A representative series of an experiment performed three times is shown [*P* values: T332D + tet versus T2A2 + tet (polio; HRV2) = 0.017; 0.026]. FLuc, firefly luciferase; HEK-293, human embryonic kidney 293; HRV2, human rhinovirus type 2; IRES, internal ribosomal entry site; LDH, lactate-dehydrogenase; RLuc, renilla luciferase.

Mnk1 activity enhances viral IRES-mediated translation

The only distinction between PV1S and PVSRIPO is the heterologous HRV2 IRES in the latter. Virus attachment and entry events do not seem to respond to oncogenic Ras in HEK-293^{Ras} cells and, thus, Mnk1 stimulation of PVSRIPO propagation most plausibly involves events following uncoating of the viral genome, *i.e.*, cap-independent translation at the heterologous IRES. We investigated the effect of Mnk1 activity on viral translation by co-transfecting uncapped, *in vitro*-transcribed subgenomic HRV2 IRES-driven renilla luciferase and conventional, m^{7}G-cap β-globin leader-driven firefly luciferase RNA reporters (**Figure 6c**). Renilla luciferase values were normalized to firefly luciferase readings to account for changes in cell number or effects on global protein synthesis due to manipulation of transfected cells. Due to the added toxicities of sustained H-Ras and RNA transfection in HEK-293^{Ras} cells and because transfection-induced stress signals to Mnk1 may interfere with our assay, we analyzed viral IRES-dependent translation in cells with controllable Mnk1 activity (**Figure 6a**).

The cell lines were tet- or mock-induced and transfected with both reporter RNAs (**Figure 6c**). The renilla luciferase:firefly luciferase ratio 8 hours post-transfection suggested that relative efficiency of cap-independent translation via the HRV2 IRES correlates with Mnk1 activity, evident as phospho-eIF4E levels (**Figure 6c**). Tet-induced dominant negative Mnk1-T2A2 had no effect on the IRES:m^{7}G-cap-dependent translation ratio, whereas Mnk1-T332D induction specifically favored cap-independent, IRES-driven translation. Phospho-eIF4E was detectable in mock-induced HEK-293^{T332D} cells, indicating active Mnk1 due to leaky Mnk1-T332D expression (**Figure 6c**). Accordingly, the IRES:m^{7}G-cap ratio suggested favorable conditions for cap-independent translation even in uninduced HEK-293^{T332D} versus HEK-293^{T2A2} cells (**Figure 6c**). This trend was further enhanced with elevated Mnk1 activity in tet-induced HEK-293^{T332D} cells (**Figure 6a**).

We tested whether the same is true for the PV IRES, which translates more efficiently in HEK-293 cells compared to its HRV2 counterpart, possibly mirroring enhanced proliferation of PV1S versus PVSRIPO. Both IRESes exhibited comparable stimulation in tet-induced HEK-293^{T332D} versus HEK-293^{T2A2} cells (**Figure 6d**). Overall, the degree of stimulation of cap-independent reporter translation by Mnk1 activity was modest. However, moderately enhanced performance of the PV1S IRES versus its HRV2 counterpart (**Figure 6d**) correlates with substantially improved viral propagation in mock-induced HEK-293^{Ras} cells (**Figure 4**). Next, we examined the effect of kinase inhibitors on the IRES:m^{7}G-cap translation ratio. LY294002, significantly favored cap-independent, IRES-mediated translation in HEK-293^{T2A2} cells, an effect that was further enhanced in tet-induced HEK-293^{T332D} cells (**Figure 6d**). This finding reflects the effects of PI3K inhibition on PVSRIPO translation, growth, and cytotoxicity in U-118 cells and oncolysis *in vivo* (**Figures 1b** and **2**) or in tet-induced HEK-293^{Ras} cells (**Figure 4d**). In contrast, Mnk1 inhibition with CGP57380 abolished stimulation of IRES-mediated translation in tet-induced HEK-293^{T332D} cells, reducing the IRES:m^{7}G-cap ratio to levels comparable to HEK-293^{T2A2} cells (**Figure 6d**). Our data suggest that MAPK control over PVSRIPO translation and replication is mediated by Mnk1 signaling and its effects on viral IRES-mediated translation.

DISCUSSION

Our studies implicate convergent Erk1/2 and p38-MAPKs signals to Mnk1 in PVSRIPO growth and cytotoxicity in GBM. PVSRIPO translation and replication in naturally susceptible U-118 glioma cells or in HEK-293 cells expressing oncogenic H-Ras strictly correlate with eIF4E phosphorylation. Similarly, only protein kinase inhibitors that block eIF4E phosphorylation inhibit PVSRIPO growth. Kinase inhibitors, such as CGP57380, are notorious for unintended effects on multiple targets, but we confirmed a role for Mnk1 in PVSRIPO growth and cytotoxicity directly in cells stably expressing mutant forms of Mnk1.

Mnk1 phosphorylation of eIF4E has been implicated in translation control of DNA virus infections, *e.g.*, herpes simplex[28] or African swine fever,[29] but its effect on translation of viral transcripts has not been defined. The role of MAPK signals in viral propagation has also been investigated with oncolytic viruses. For example, Ras/Erk1/2 signaling may mediate tumor cell-specific cytotoxicity of reovirus,[30] or vesicular stomatitis virus (VSV).[31] The latter is pertinent here, because VSV oncolysis-like PVSRIPO-benefits from simultaneous mTOR inhibition.[32] VSV, highly sensitive to interferon defenses, exhibits conditional replication in tumor cells with defective interferon response. Ras/MAPK and mTOR signals have been linked to suppressive and supportive roles in interferon signaling, respectively, explaining their role in VSV oncolysis.[32]

Therefore, it is possible that PVSRIPO tumor cytotoxicity and its response to kinase inhibitors, like VSV reflects the status of the interferon system. We do not think this is the case for the following reasons. PV:host cell interactions are dominated by drastic, very early effects on host cell gene expression. These are due to two viral proteases, 2A and 3C, which target a range of critical host cell entities such as eIF4G,[33] the poly(A) BP[34] or the nuclear pore complex.[35] Thus, PV counters innate immune responses by broadly disrupting host cell translation and nucleocytoplasmic transport early after uncoating. It can afford such radical measures, because the viral life cycle is intact in a severely compromised host cell environment. This strategy entirely depends on competitive viral, cap-independent translation immediately after release of the viral RNA into the host cytoplasm.[36] In other words, the success of the PV life cycle depends on recruiting ribosomes to incoming viral RNA and, thus, its ability to co-opt eIF4G to interact with the viral IRES.

The HRV2 IRES in PVSRIPO may be inherently deficient to carry out this critical, rate-limiting step in the normal central nervous system. Mapping the locus for HRV2 IRES incompetence in HEK-293 cells identified a discrete region within stem-loop domain 5 (ref. 3). This area, which also harbors the neuroattenuating IRES point mutations in all three Sabin strains, provides the landing pad for eIF4G in the PV IRES.[12] Overlapping determinants for HRV2 IRES central nervous system deficiency and eIF4G binding suggest a functional relationship. It also suggests that PVSRIPO translation, growth and cytotoxicity in GBM may be enabled by an environment supporting eIF4G:IRES interaction.

eIF4E, possibly a rate-limiting translation factor,[37] regulates initiation by anchoring eIF4G at the m^{7}G-cap, enabling 40S

ribosomal subunit recruitment. By controlling initiation complex formation at the m^{7}G-cap, eIF4E may in effect regulate the function of its binding partner eIF4G in cap-independent translation initiation.[20] This would suggest that eIF4E phosphorylation by Mnk may alter translation initiation complex formation on select mRNAs, either through modulating eIF4F formation at the m^{7}G-cap or eIF4G:IRES interaction. Such a role for Mnk has been difficult to establish, due to contradictory reported effects of eIF4E phosphorylation on m^{7}G–cap interactions. eIF4E phosphorylation has been variably proposed to enhance[38,39] or reduce m^{7}G-cap-binding.[40,41] Our data are consistent with reports suggesting reduced affinity of phospho-eIF4E for the m^{7}G-cap.[40,41] This may generate "free" eIF4F not committed to the m^{7}G-cap, thus enabling enhanced eIF4G:IRES association and improved PVSRIPO translation. Previous investigations of Mnk1 activation in HEK-293 cells suggested an IRES:m^{7}G-cap ratio altered in favor of cap-independent initiation, similar to our findings.[42] Eukaryotic IRES-competent mRNAs may initiate translation via eIF4G binding[13] and, thus, respond to mitogenic signals similar to PVSRIPO. We do not make such a claim, mainly because the exceeding structural complexity, heterogeneity, and functional plasticity of eukaryotic mRNAs preclude such simple predictions. In its simplicity, PVSRIPO is a unique sensor of translation factor function in cancer, because the viral RNA lacks an m^{7}G-cap and viral translation categorically depends on eIF4G:IRES interaction for cap-independent 40S subunit recruitment.

We observed stimulation of viral, cap-independent translation, PVSRIPO growth, and cytotoxicity upon PI3K inhibition. It has been reported previously that mTOR inhibition resulting in 4E-BP phosphorylation stimulates viral IRES-mediated translation.[20] Parallel to our hypothesis regarding the role of Mnk1 and eIF4E phosphorylation in PVSRIPO oncolysis, it has been proposed that "decommissioning" eIF4G from m^{7}G-cap binding (in this case by promoting 4E-BP-mediated dissociation from eIF4E) stimulates cap-independent translation.[20] Based on these findings, there is compelling molecular correlative evidence for synergistic combination of PVSRIPO with inhibitors of PI3K/mTOR. Indeed, our studies document accelerated tumor-cell killing and xenograft regression when combining PVSRIPO with the PI3K inhibitor LY294002 *in vivo*.

MATERIALS AND METHODS

Viruses, cells, tet-inducible cell lines. PVSRIPO is the live attenuated PV serotype 1 (Sabin) (GenBank accession no. V01150) containing a heterologous IRES of HRV2 (GenBank accession no. X02316). Construction of PVSRIPO as well as propagation and purification of PVSRIPO and PV1S stocks have been described previously.[1,3,5] U-118 cells (ATCC) were propagated according to the provider's instructions. Tet-inducible HEK-293^{Ras}, HEK-293^{T332D}, HEK-293^{T2A2} cells, based on the Flp-In TREx 293 line (Invitrogen), were grown in Dulbecco's modified Eagle medium (DMEM), 10% fetal calf serum (-tet) (Invitrogen), 100 µg/ml zeocin, and 15 µg/ml blasticidin. HEK-293^{Ras} cells were generated with a PCR fragment obtained with primers 5′-aaggatccgacaagacggaatataagctt and 5′-aactcgagt caggagagcacacacttgcag from V12 H-Ras complementary DNA and cloned in frame into the FRP-Myc plasmid13 placing it under CMV/TetO2 promoter control and providing hygromycin resistance. The mutant Mnk1 ORFs were excised from pEBG-Mnk1(T332D/T2A2)18 with *BamH*1 and cloned into the pcDNA5/FRT/TO plasmid creating FRP-T332D/-T2A2. Flp-In TREx cells were co-transfected with 0.1 µg FRP-myc-Ras, FRP-T332D, FRP-T2A2 or vector (EF6) + 1 µg pOG44 (expressing the Flp recombinase). Selection with hygromycin and blasticidin was performed according to the manufacturer's instructions. All assays were performed with cells at passage <10.

Immunoblots and kinase inhibitors. Cells were washed with PBS and scraped in lysis buffer [10% glycerol, 50 mmol/l HEPES, 1 mmol/l EDTA, 5 mmol/l EGTA, 150 mmol/l NaCl, 0.5% NP40, protease inhibitor (complete EDTA free; Roche Diagnostics, Indianapolis, IN), Halt-phosphatase inhibitor (Thermo Scientific, Waltham, MA)]. Twenty microgram of total protein was loaded per well of 4–12% Bis–Tris gel (NuPage; Invitrogen) and separated at 150 V for 75 minutes. Proteins were transferred to nitrocellulose membrane (Protran; Whatman, Piscataway, NJ) at 4 °C in transfer buffer (150 mmol/l glycin, 20 mmol/l Tris-HCl, 20% methanol). Membranes were blocked overnight in blocking solution (Starting Block; Thermo Scientific) and incubated with primary antibody for 1 hour at room temperature (RT), washed three times with TPBS (PBS containing 0.5% Tween-20) and incubated with secondary antispecies antibody for 1 hour at RT. Membranes were washed again three times with TPBS and developed with chemiluminescence reagent (Super Signal West Pico; Thermo Scientific) on HyBlot CL film (Denville, Metuchen, NJ). Antibodies against the following antigens were used according to the manufacturers specifications: Akt, p-Akt(Ser473), S6, p-S6(Ser240/244), eIF4E, p-eIF4E(Ser209), eIF4G, p-eIF4G(Ser1108), Erk1/2, p-Erk1/2 (Thr202/Tyr204), p38-MAPK(Thr180/182), 4E-BP, p-4EBP (Thr36/47), Mnk1, and p-Mnk1 (Thr197/202) (Cell Signaling Technology, Danvers, MA) and c-*myc* (Sigma, St Louis, MO). Kinase inhibitors in this study include LY294002, UO126 (Cell Signaling Technology) and CGP57380 (Calbiochem, Gibbstown, NJ) used at the concentrations indicated in figures or figure legends. Tet induction was carried out with 1 mg/ml tet in 100% ethanol as 1:1,000 stock solution for the indicated intervals. Inhibitors were added 2 hours before cells were processed.

Cells, infections, and one-step growth curves. HEK-293 and U-118 cells were maintained in DMEM (Invitrogen), supplemented with 10% fetal calf serum at 37 °C in 5% CO_2. To determine viral replication kinetics, ~90% confluent monolayers (consisting of ~5 × 10^5 cells) in 35 mm dishes were overlaid with DMEM-containing virus at an MOI as indicated. Subsequently, plates were rocked for 30 minutes at RT. Cells were then washed three times with serum-free DMEM to remove unbound virus particles and covered with DMEM supplemented with 2% fetal bovine serum. Infected cells were incubated at 37 °C and were lysed at the indicated intervals by two freeze/thaw cycles. Viral titers were quantified by plaque assay on HeLa cells as described before.[3]

Cytotoxicity assay. Ten thousand U-118, HEK-293^{Ras}, or HEK-293$^{T332D/T2A2}$ cells were plated in 100 µl DMEM (-sodium pyruvate) (Invitrogen) in 96-well plates. PVSRIPO at various MOI was added to the wells and the cells were incubated for the indicated intervals at 37 °C. Cytotoxicity was analyzed with the lactate-dehydrogenase-cytotocixity plus kit (Roche Diagnostics) and quantified with a Genios plate reader (Tecan, Durham, NC) at 492 nm. If required, tet/vehicle or kinase inhibitors were added 6 hours or 2 hours before the cells, respectively. To enable normalization of values, "low" (native cells) and "lysed" (cells treated with the manufacturer-provided lysis buffer) standards were obtained and used in the following formula: [(value-low)/(lysed-low)] × 100. Due to instability of lactate-dehydrogenase released from infected cells, the extent of cell death might be significantly higher than suggested by this formula, especially after prolonged incubation. Values shown are representative for experiments performed in triplicate and repeated at least twice.

Mouse xenograft studies, histology, virus recovery from xenografts. All vertebrate animal procedures were carried out with approval of the Institutional Animal Care and Use Committee. Flank U-118 xenografts were established by depositing 6 × 10^6 cells subcutaneously in 8-week

old, female athymic Balb/c mice (bred in-house) as described before.[5] Intratumoral PVSRIPO/vehicle injections were carried out as described in detail previously.[5] LY294002 was dissolved in dimethyl sulfoxide and injected intraperitoneally at a dose of 25 µg/g. The total volume of dimethyl sulfoxide administered daily was 1 µl/g. Tumors were measured by Vernier caliper in 5-day intervals and their size was calculated as follows: $v = (\text{length}) \times (\text{width})^2 \times (\pi/6)$. Animals were euthanized with intraperitoneal pentobarbital (250 mg/kg), perfused with PBS and their carcasses processed for dissection of xenograft tissues. Dissected tumor tissues were fixed in 4% neutral-buffered paraformaldehyde (in PBS) for 2 hours at RT and processed for paraffin embedding, sectioning at 20 µm and hematoxylin and eosin staining as described before.[5] For PVSRIPO recovery, xenograft tissues were immersed in 750 µl DMEM and thoroughly dounced in microtissue grinders (Potter-Elvejhem). The resulting slurry was briefly centrifuged to remove large debris and the homogenate was serially diluted and used in a standard plaque assay as described.[5]

Real time-PCR. To analyze virus entry, mock-/tet-induced HEK-293^{Ras} cells were rinsed with PBS, scraped, pelleted, and incubated in hypotonic buffer (25 mmol/l HEPES, 400 mmol/l KOAc, 15 mmol/l $Mg(OAc)_2$, 2% digitonin, 1 mmol/l dithiothreitol) for 5 minutes at 4 °C. The lysate was dounce-homogenized and centrifuged to separate the membrane-enriched pellet and supernatant comprising the cytosolic compartment. Real time-PCR was performed as described before.

RNA reporters. RNA reporters, constructed as described,[43] were *in vitro*-transcribed using the T7 Message Machine Kit or T7 Megascript Kit (Applied Biosystems, Foster City, CA) for m^7G-cap-equipped/uncapped RNA reporters, respectively. One million of the respective tet-inducible HEK-293 cells were co-transfected with 1-µg IRES-dependent RNA reporter and 0.5-µg cap-dependent RNA. RNA transfections were performed by mixing *in vitro* transcript RNA and 5 µl DMRIEC (Invitrogen) transfection reagent in 100 µl OPTI-MEM (Invitrogen). At 8 hours post-transfection, cells were washed in PBS and scraped into 100 µl lysis buffer. Luminometer readings were performed with 10 µl lysate in a GloMax20/20n luminometer (Turner, Madison, WI) using the Dual Luciferase Reporter Assay System (Promega, Madison, WI) according to the manufacturer's specifications. HEK-293^{T332D} or HEK-293^{T2A2} cells were mock- or tet-induced for 6 hours, and inhibitors, if indicated, were added 2 hours before RNA transfection.

ACKNOWLEDGMENTS

We thank the laboratories of Drs Rich (Duke University Medical Center) and Cooper (Fred Hutchinson Cancer Research Center) for generously sharing H-Ras and Mnk expression clones. We are also thankful for generous access to the ELISA plate reader to Dr Bigner (Duke University Medical Center), S. Bradrick, and E. Dobrikova for sharing complementary DNA constructs and cell lines and M. Shveygert and S. Bradrick for critical reading of our manuscript. This work was supported by PHS grants CA124756 and CA140510 (M.G.) and a grant from Alex's Lemonade Stand Foundation.

REFERENCES

1. Gromeier, M, Lachmann, S, Rosenfeld, MR, Gutin, PH and Wimmer, E (2000). Intergeneric poliovirus recombinants for the treatment of malignant glioma. *Proc Natl Acad Sci USA* **97**: 6803–6808.
2. Gromeier, M, Alexander, L and Wimmer, E (1996). Internal ribosomal entry site substitution eliminates neurovirulence in intergeneric poliovirus recombinants. *Proc Natl Acad Sci USA* **93**: 2370–2375.
3. Campbell, SA, Lin, J, Dobrikova, EY and Gromeier, M (2005). Genetic determinants of cell type-specific poliovirus propagation in HEK 293 cells. *J Virol* **79**: 6281–6290.
4. Yang, X, Chen, E, Jiang, H, Muszynski, K, Harris, RD, Giardina, SL *et al.* (2009). Evaluation of IRES-mediated, cell-type-specific cytotoxicity of poliovirus using a colorimetric cell proliferation assay. *J Virol Methods* **155**: 44–54.
5. Dobrikova, EY, Broadt, T, Poiley-Nelson, J, Yang, X, Soman, G, Giardina, S *et al.* (2008). Recombinant oncolytic poliovirus eliminates glioma *in vivo* without genetic adaptation to a pathogenic phenotype. *Mol Ther* **16**: 1865–1872.
6. Sonenberg, N, Morgan, MA, Merrick, WC and Shatkin, AJ (1978). A polypeptide in eukaryotic initiation factors that crosslinks specifically to the 5′-terminal cap in mRNA. *Proc Natl Acad Sci USA* **75**: 4843–4847.
7. Morley, SJ, Curtis, PS and Pain, VM (1997). eIF4G: translation's mystery factor begins to yield its secrets. *RNA* **3**: 1085–1104.
8. Hentze, MW (1997). eIF4G: a multipurpose ribosome adapter? *Science* **275**: 500–501.
9. Pelletier, J and Sonenberg, N (1988). Internal initiation of translation of eukaryotic mRNA directed by a sequence derived from poliovirus RNA. *Nature* **334**: 320–325.
10. Jang, SK, Kräusslich, HG, Nicklin, MJ, Duke, GM, Palmenberg, AC and Wimmer, E (1988). A segment of the 5′ nontranslated region of encephalomyocarditis virus RNA directs internal entry of ribosomes during *in vitro* translation. *J Virol* **62**: 2636–2643.
11. Nomoto, A, Lee, YF and Wimmer, E (1976). The 5′ end of poliovirus mRNA is not capped with m7G(5′)ppp(5′)Np. *Proc Natl Acad Sci USA* **73**: 375–380.
12. de Breyne, S, Yu, Y, Unbehaun, A, Pestova, TV and Hellen, CU (2009). Direct functional interaction of initiation factor eIF4G with type 1 internal ribosomal entry sites. *Proc Natl Acad Sci* **37**: 5167–5182.
13. Kaiser, C, Dobrikova, EY, Bradrick, SS, Shveygert, M, Herbert, JT and Gromeier, M (2008). Activation of cap-independent translation by variant eukaryotic initiation factor 4G in vivo. *RNA* **14**: 2170–2182.
14. Pause, A, Belsham, GJ, Gingras, AC, Donzé, O, Lin, TA, Lawrence, JC Jr *et al.* (1994). Insulin-dependent stimulation of protein synthesis by phosphorylation of a regulator of 5′-cap function. *Nature* **371**: 762–767.
15. Raught, B, Gingras, AC, Gygi, SP, Imataka, H, Morino, S, Gradi, A *et al.* (2000). Serum-stimulated, rapamycin-sensitive phosphorylation sites in the eukaryotic translation initiation factor 4GI. *EMBO J* **19**: 434–444.
16. Beretta, L, Gingras, AC, Svitkin, YV, Hall, MN and Sonenberg, N (1996). Rapamycin blocks the phosphorylation of 4E-BP1 and inhibits cap-dependent initiation of translation. *EMBO J* **15**: 658–664.
17. Fukunaga, R and Hunter, T (1997). MNK1, a new MAP kinase-activated protein kinase, isolated by a novel expression screening method for identifying protein kinase substrates. *EMBO J* **16**: 1921–1933.
18. Waskiewicz, AJ, Flynn, A, Proud, CG and Cooper, JA (1997). Mitogen-activated protein kinases activate the serine/threonine kinases Mnk1 and Mnk2. *EMBO J* **16**: 1909–1920.
19. Pyronnet, S, Imataka, H, Gingras, AC, Fukunaga, R, Hunter, T and Sonenberg, N (1999). Human eukaryotic translation initiation factor 4G (eIF4G) recruits mnk1 to phosphorylate eIF4E. *EMBO J* **18**: 270–279.
20. Svitkin, YV, Herdy, B, Costa-Mattioli, M, Gingras, AC, Raught, B and Sonenberg, N (2005). Eukaryotic translation initiation factor 4E availability controls the switch between cap-dependent and internal ribosomal entry site-mediated translation. *Mol Cell Biol* **25**: 10556–10565.
21. Cancer Genome Atlas Research Network (2008). Comprehensive genomic characterization defines human glioblastoma genes and core pathways. *Nature* **455**: 1061–1068.
22. Gupta, AK, Cerniglia, GJ, Mick, R, Ahmed, MS, Bakanauskas, VJ, Muschel, RJ *et al.* (2003). Radiation sensitization of human cancer cells *in vivo* by inhibiting the activity of PI3K using LY294002. *Int J Radiat Oncol Biol Phys* **56**: 846–853.
23. Fan, QW, Specht, KM, Zhang, C, Goldenberg, DD, Shokat, KM and Weiss, WA (2003). Combinatorial efficacy achieved through two-point blockade within a signaling pathway-a chemical genetic approach. *Cancer Res* **63**: 8930–8938.
24. Liu, TC, Wakimoto, H, Martuza, RL and Rabkin, SD (2007). Herpes simplex virus Us3(-) mutant as oncolytic strategy and synergizes with phosphatidylinositol 3-kinase-Akt targeting molecular therapeutics. *Clin Cancer Res* **13**: 5897–5902.
25. Merrill, MK and Gromeier, M (2006). The double-stranded RNA binding protein 76:NF45 heterodimer inhibits translation initiation at the rhinovirus type 2 internal ribosome entry site. *J Virol* **80**: 6936–6942.
26. Ueda, T, Watanabe-Fukunaga, R, Fukuyama, H, Nagata, S and Fukunaga, R (2004). Mnk2 and Mnk1 are essential for constitutive and inducible phosphorylation of eukaryotic initiation factor 4E but not for cell growth or development. *Mol Cell Biol* **24**: 6539–6549.
27. Hirota, T, Irie, K, Okamoto, R, Ikeda, W and Takai, Y (2005). Transcriptional activation of the mouse Necl-5/Tage4/PVR/CD155 gene by fibroblast growth factor or oncogenic Ras through the Raf-MEK-ERK-AP-1 pathway. *Oncogene* **24**: 2229–2235.
28. Walsh, D and Mohr, I (2004). Phosphorylation of eIF4E by Mnk-1 enhances HSV-1 translation and replication in quiescent cells. *Genes Dev* **18**: 660–672.
29. Castelló, A, Quintas, A, Sánchez, EG, Sabina, P, Nogal, M, Carrasco, L *et al.* (2009). Regulation of host translational machinery by African swine fever virus. *PLoS Pathog* **5**: e1000562.
30. Coffey, MC, Strong, JE, Forsyth, PA and Lee, PW (1998). Reovirus therapy of tumors with activated Ras pathway. *Science* **282**: 1332–1334.
31. Noser, JA, Mael, AA, Sakuma, R, Ohmine, S, Marcato, P, Lee, PW *et al.* (2007). The RAS/Raf1/MEK/ERK signaling pathway facilitates VSV-mediated oncolysis: implication for the defective interferon response in cancer cells. *Mol Ther* **15**: 1531–1536.
32. Alain, T, Lun, X, Martineau, Y, Sean, P, Pulendran, B, Petroulakis, E *et al.* (2010). Vesicular stomatitis virus oncolysis is potentiated by impairing mTORC1-dependent type I IFN production. *Proc Natl Acad Sci USA* **107**: 1576–1581.
33. Etchison, D, Milburn, SC, Edery, I, Sonenberg, N and Hershey, JW (1982). Inhibition of HeLa cell protein synthesis following poliovirus infection correlates with the proteolysis of a 220,000-dalton polypeptide associated with eucaryotic initiation factor 3 and a cap binding protein complex. *J Biol Chem* **257**: 14806–14810.
34. Kuyumcu-Martinez, NM, Van Eden, ME, Younan, P and Lloyd, RE (2004). Cleavage of poly(A)-binding protein by poliovirus 3C protease inhibits host cell translation: a novel mechanism for host translation shutoff. *Mol Cell Biol* **24**: 1779–1790.
35. Gustin, KE and Sarnow, P (2001). Effects of poliovirus infection on nucleo-cytoplasmic trafficking and nuclear pore complex composition. *EMBO J* **20**: 240–249.

36. Dobrikova, EY, Grisham, RN, Kaiser, C, Lin, J and Gromeier, M (2006). Competitive translation efficiency at the picornavirus type 1 internal ribosome entry site facilitated by viral cis and trans factors. *J Virol* **80**: 3310–3321.
37. Duncan, R, Milburn, SC and Hershey, JW (1987). Regulated phosphorylation and low abundance of HeLa cell initiation factor eIF-4F suggest a role in translational control. Heat shock effects on eIF-4F. *J Biol Chem* **262**: 380–388.
38. Marcotrigiano, J, Gingras, AC, Sonenberg, N and Burley, SK (1997). Cocrystal structure of the messenger RNA 5′ cap-binding protein (eIF4E) bound to 7-methyl-GDP. *Cell* **89**: 951–961.
39. Minich, WB, Balasta, ML, Goss, DJ and Rhoads, RE (1994). Chromatographic resolution of *in vivo* phosphorylated and nonphosphorylated eukaryotic translation initiation factor eIF-4E: increased cap affinity of the phosphorylated form. *Proc Natl Acad Sci USA* **91**: 7668–7672.
40. Scheper, GC, van Kollenburg, B, Hu, J, Luo, Y, Goss, DJ and Proud, CG (2002). Phosphorylation of eukaryotic initiation factor 4E markedly reduces its affinity for capped mRNA. *J Biol Chem* **277**: 3303–3309.
41. Slepenkov, SV, Darzynkiewicz, E and Rhoads, RE (2006). Stopped-flow kinetic analysis of eIF4E and phosphorylated eIF4E binding to cap analogs and capped oligoribonucleotides: evidence for a one-step binding mechanism. *J Biol Chem* **281**: 14927–14938.
42. Knauf, U, Tschopp, C and Gram, H (2001). Negative regulation of protein translation by mitogen-activated protein kinase-interacting kinases 1 and 2. *Mol Cell Biol* **21**: 5500–5511.
43. Florez de Sessions, P, Dobrikova, E and Gromeier, M (2007). Genetic adaptation to untranslated region-mediated enterovirus growth deficits by mutations in the nonstructural proteins 3AB and 3CD. *J Virol* **81**: 8396–8405.